Food Chemistry 196 (2016) 935–942

Contents lists available at ScienceDirect

Food Chemistry

journal homepage: www.elsevier.com/locate/foodchem

An integrated approach with experimental and computational tools outlining the cooperative binding between 2-phenylchromone and human serum albumin

Ícaro Putinhon Caruso [a,b], José Maria Barbosa Filho [c], Alexandre Suman de Araújo [b], Fátima Pereira de Souza [a,b], Marcelo Andrés Fossey [a,b], Marinônio Lopes Cornélio [a,b,*]

[a] Departamento de Física, Instituto de Biociências, Letras e Ciências Exatas (IBILCE), UNESP, Rua Cristovão Colombo 2265, CEP 15054-000 São José do Rio Preto, SP, Brazil
[b] Centro Multiusuário de Inovação Biomolecular (CMIB), Instituto de Biociências, Letras e Ciências Exatas (IBILCE), UNESP, Rua Cristovão Colombo 2265, CEP 15054-000 São José do Rio Preto, SP, Brazil
[c] Laboratório de Tecnologia Famacêutica (LTF), UFPB, Cidade Universitária, CEP 58051-900 João Pessoa, PB, Brazil

ARTICLE INFO

Article history:
Received 17 April 2015
Received in revised form 1 September 2015
Accepted 7 October 2015
Available online 9 October 2015

Keywords:
2-Phenylchromone
Human serum albumin
Fluorescence spectroscopy
Binding density function
Cooperative binding
Computational methods

ABSTRACT

2-Phenylchromone (2PHE) is a flavone, found in cereals and herbs, indispensable in the human diet. Its chemical structure is the basis of all flavonoids present in black and green tea, soybean, red fruits and so on. Although offering such nutritional value, it still requires a molecular approach to understand its interactions with a specific target. The combination of experimental and computational techniques makes it possible to describe the interaction between 2PHE and human serum albumin (HSA). Fluorescence spectroscopy results show that the quenching mechanism is static, and thermodynamic analysis points to an entropically driven complex. The binding density function method provides information about a positive cooperative interaction, while drug displacement experiments indicate Sites 1 and 2 of HSA as the most probable binding sites. From the molecular dynamic study, it appears that the molecular docking is in agreement with experimental data and thus more realistic.

1. Introduction

Flavonoids are polyphenolic secondary metabolites that are widely distributed in higher plants and are ingested by humans in their food (Bravo, 1998). They have attracted considerable attention in the scientific community, owing to a biological and physiological interest. The literature shows that flavonoids can present antioxidant, anticancer, antiviral, anti-inflammatory and heart disease protective activities (Grotewold, 2006). Flavones are one of the major classes of flavonoids, and are mainly found in cereals and herbs (Bravo, 1998). 2-Phenylchromone (2PHE) is a flavone which has the basic structure of all flavonoids, as shown in Fig. 1a. In addition to its antioxidant activity, 2PHE also exhibits the inhibitory property of estrogen without binding to the estrogen receptor, but acting as a competitive agonist for the aryl hydrocarbon receptor, which means that it is anti-estrogenic flavonoid (Jung, Ishida, Nishikawa, & Nishihara, 2007). 2PHE present in *Primula macrophylla* (Primulaceae) is the major compound responsible for the antileishmanial activity of the plant (Najmus-Saqib, Alam, & Ahmad, 2009).

Human serum albumin (HSA) is the main extracellular protein, and is highly concentrated, in blood plasma. HSA is a monomeric globular protein composed of three structurally similar domains (I, II and III), each containing two subdomains (A and B). Aromatic and heterocyclic ligands bind to HSA primarily within two hydrophobic pockets in subdomains IIA and IIIA, namely Sites 1 and 2, respectively. Site 1 is the primary binding site for drugs like warfarin and phenylbutazone analogs, whereas diazepam and ibuprofen are bound primarily to Site 2 (Peters, 1996). Studies have indicated that the subdomain IB can also be a binding site for compounds such as bilirubin, hemin and methyl orange. Subdomain IB has been called Site 3 (Zsila, 2013). The exceptional capacity of HSA to interact with several organic and inorganic molecules turns this protein into an important regulator of intercellular fluxes and the main carrier for many drugs to different molecular targets. Up until now most of the studies with several kinds of flavonoids (Caruso, Vilegas, Fossey, & Cornélio, 2012; Caruso, Vilegas, Souza, Fossey,

* Corresponding author at: Departamento de Física, Instituto de Biociências, Letras e Ciências Exatas (IBILCE), UNESP, Rua Cristovão Colombo 2265, CEP 15054-000 São José do Rio Preto, SP, Brazil.
E-mail addresses: ykrocaruso@hotmail.com (Í.P Caruso), jbarbosa@ltf.ufpb.br (J.M.B. Filho), asaraujo@ibilce.unesp.br (A.S. de Araújo), fatima@ibilce.unesp.br (F.P. de Souza), marcelo@ibilce.unesp.br (M.A. Fossey), mario@ibilce.unesp.br (M.L. Cornélio).

http://dx.doi.org/10.1016/j.foodchem.2015.10.027
0308-8146/

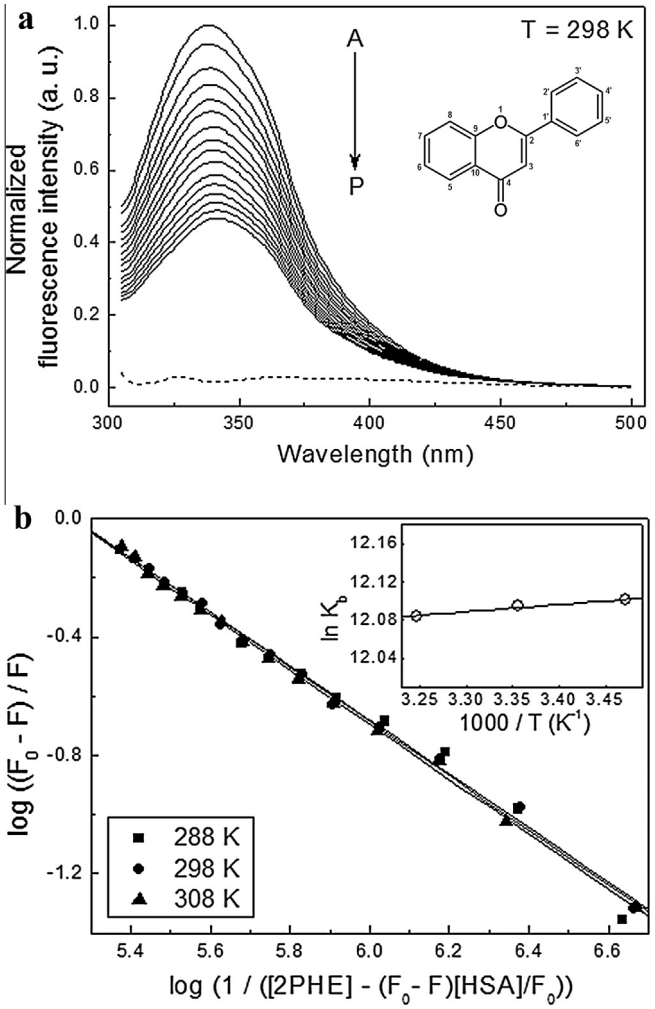

Fig. 1. (a) Emission spectra of HSA obtained with the increments of the 2PHE concentration (pH 7.0, T = 298 K, λ_{ex} = 295 nm). [HSA] = 4.0 μM; [2PHE] (μM), A–P: from 0 to 6.0 with the increments of 0.4. The dotted line corresponds to the emission spectrum of 2PHE in phosphate buffer (6.0 μM). The insert corresponds to the chemical structure of 2-phenylchromone. (b) Double-log plots for the fluorescence quenching of HSA by 2PHE at pH 7.0 and 288, 298 and 308 K. The insert corresponds to the van't Hoff plot for the HSA–2PHE complex.

& Cornélio, 2014; Peters, 1996; Sinisi, Forzato, Cefarin, Navarini, & Berti, 2015; Wu, Yan, Wang, Wang, & Li, 2015) investigating the mechanism of interaction have identified a single binding site. Therefore, a more detailed study of the microenvironment of the binding sites of HSA is important in order to achieve a better comprehension of this mechanism.

This paper presents a broad and detailed study on the interaction between the polyphenolic compound considered to be the basic structure of flavonoids (2PHE) and the principal carrier protein in human blood plasma (HSA). The formation of the HSA–2PHE complex was investigated using spectroscopy methods including fluorescence spectroscopy, UV–Vis absorbance, circular dichroism (CD), and computational methods like *ab initio*, molecular dynamic and docking calculations. In particular, this work also made use of the binding density function (BDF) method for data analysis of fluorescence quenching, which is very sparsely explored in the study of protein–ligand interactions. This data set may contribute scientifically to a better understanding of the interaction mechanisms involved in the formation of the protein–flavonoid complex, and the distribution and transportation of flavonoids, which is an important research field in food chemistry.

2. Materials and methods

2.1. Materials and solutions

Human serum albumin fraction V, 2-phenylchromone, warfarin, ibuprofen, methyl orange, dibasic sodium phosphate, citric acid, ethanol and sodium chloride (NaCl) were purchased from Sigma Chemical Co. All other chemicals were of analytical reagent grade and Milli-Q ultrapure water was used throughout the experiments. HSA was dissolved in a phosphate buffer solution of 50 mM at pH 7.0, and adjusted with citric acid, containing 0.15 M of NaCl. The stock solution of 2PHE was prepared in absolute ethanol. The concentrations of the stock solutions of HSA and 2PHE were determined spectroscopically using the molar extinction coefficient of 36,500 and 25,100 $M^{-1}cm^{-1}$ at 280 and 294 nm, respectively. Aliquots of 2PHE applied in the following experiments were carefully evaluated to avoid aggregation of the flavonoid (Pohjala & Tammela, 2012).

2.2. UV–Vis absorbance spectroscopy

UV–Vis absorption spectrum was recorded at room temperature (298 K), controlled by air conditioning and monitored by a thermometer, on a Cary-3E spectrophotometer (Varian, Palo Alto, CA) equipped with a quartz cell with 1.0 cm optical path length. UV–Vis absorption spectra were recorded in the 250–500 nm range, with an integration time of 0.333 s and a spectral bandwidth of 2.0 nm.

2.3. Fluorescence spectroscopy

The fluorescence measurements were performed using an ISS PC1 steady-state spectrofluorimeter (Champaign, IL, USA) equipped with a quartz cell with 1.0 cm optical path length and a Neslab RTE-221 thermostat bath. Both excitation and emission bandwidths were set at 8.0 nm. The excitation wavelength of 295 nm was chosen since it provides no excitation of tyrosine residues, but excites the single tryptophan residue (Trp214) of HSA (Lakowicz, 1999). The emission spectrum was collected in the range of 305–500 nm with increments of 1.0 nm, which was corrected for the background fluorescence of the buffer and for inner filter effects (Borissevitch, 1999). Each point in the emission spectrum is the average of 10 accumulations. In the fluorescence quenching experiments, titrations were performed by adding small aliquots from the 2PHE stock solution to the HSA solution (3.0 ml) at constant concentrations of 1.0, 2.0 and 4.0 μM. In experiments for Stern–Volmer and binding equilibria analysis, the HSA concentration remained constant at 4.0 μM, and the 2PHE concentration varied from 0 to 6.0 μM with increments of 0.4 μM at 288, 298 and 308 K. For the binding density function (BDF) method, the titration was performed at HSA constant concentrations of 1.0, 2.0 and 4.0 μM, and the 2PHE concentration varied from 0 to 2.8, 3.6 and 6.0 μM, respectively, at 298 K. The effect of ethanol as a co-solvent was verified by adding small aliquots to the HSA solution (4.0 μM at 3.0 ml, 298 K) within the volume changes of the previous titrations. In all experiments, the final volume of ethanol in the buffer was <1%.

2.4. Drug displacement experiment

Site-specific marker displacement experiments were carried out by titrating complexes of HSA (4.0 μM at 298 K) with warfarin, ibuprofen and methyl orange at molar ratios of 1:0 and 1:1, with the 2PHE concentration increasing from 0 to 8.0 μM in increments of 1.0 μM. Warfarin, ibuprofen and methyl orange are site-specific

markers that bind to HSA at subdomain IIA (Site 1), IIIA (Site 2) and IB (Site 3), respectively (Peters, 1996; Zsila, 2013). The fluorescence quenching experiments of HSA by 2PHE in the absence and presence of site-specific markers were performed using the same method in the previous section (Section 2.3).

2.5. UV circular dichroism spectroscopy

UV CD spectra were recorded at room temperature on a Jasco J-710 spectropolarimeter equipped with a demountable quartz cell with a 0.01 cm optical path length, model DRC-H (Jasco, USA). The UV CD spectra were recorded in the 190–260 nm range with a scan rate 20 nm/min and a spectral resolution of 0.1 nm. For each spectrum 10 accumulations were performed. The HSA concentration remained constant throughout the experiment at 4.0 μM, while the 2PHE to HSA ratios were 0:1, 1:1 and 2:1. The contribution of the CD spectrum to the buffer and the 2PHE was subtracted from free and complexed HSA. All CD spectra were taken as millidegrees (θ) and subsequently expressed in terms of mean residue ellipticity (MRE or [Θ]) in deg cm^2 dmol^{-1} using the following equation:

$$[\Theta] = \theta(m\,\mathrm{deg})/(10\ [P]\ l\ n) \quad (1)$$

where [P] is the molar concentration of the protein (HSA), n is the quantity of amino acid residues (585), and l is the optical path length (cm). Secondary structures were estimated with CONTINLL software from the CDPro package, using the reference set of proteins SMP56 (Sreerama & Woody, 2000). The effect of ethanol as a co-solvent was verified by adding an aliquot to the HSA solution (4.0 μM at 3.0 ml, 298 K) within the volume change of the last titration. In all experiments, the final volume of ethanol in the buffer was <1%.

2.6. Ab initio calculation

The Gaussian 09 program (Frisch et al., 2009) provided by the Núcleo de Computação Científica da Universidade Estadual Paulista (NCC/GridUNESP) was applied to the calculation of the 2PHE structure. The optimized geometry calculated at the gas phase with the 2PHE molecule isolated by the DFT/B3LYP/6-311++G(2d,p) method. The next step, the vibrational frequency calculation, was performed to check the optimized 2PHE molecule. The TD-DFT/B3LYP/6-311+G(d,p) calculation was performed with the optimized 2PHE, taking into account all excitations from the 9 highest occupied molecular orbitals (HOMOs) to the 9 lowest unoccupied molecular orbitals (LUMOs). The solvent effect in ethanol was verified using the PCM calculation (Mennucci, Cancès, & Tomasi, 1997). The molecular electrostatic potential (MEP) map was calculated to investigate the distribution of charge density on the molecular surface of 2PHE.

2.7. Molecular dynamic calculation

All the molecular dynamic (MD) simulations were performed with the NAMD 2.9 program (Phillips et al., 2005). The molecular system was modeled with the CHARMM36 force field (Best et al., 2012) and TIP3P water model (Jorgensen, Chandrasekhar, Madura, Impey, & Klein, 1983). The crystal structure of HSA at a 2.5 Å resolution (PDB-ID: 1AO6) (Sugio, Kashima, Mochikuzi, Noda, & Kobayashi, 1999) was placed in the center of a 100 Å cubic box solvated by a solution of 0.15 M of NaCl in water, and the protonation state of ionizable residues was set considering a neutral pH (pH = 7.0). Periodic boundary conditions were used and all simulations were performed in NPT ensemble. The temperature was kept constant at 298 K using Langevin dynamics with a damping coefficient of 1 ps^{-1}. The pressure was maintained at 1 atm by a Nose–Hoover Langevin piston, with a piston period of 200 fs, a damping time scale of 100 fs and a barostat noise temperature of 298 K. The cutoff for small-range interactions was set to 12 Å, with a switch distance of 10 Å and a pair list distance of 14 Å. The long-range electrostatic interactions were calculated using the particle mesh Ewald (PME) algorithm. In every MD simulation a time step of 2 fs was used and all covalent bonds involving hydrogen atoms were constrained to their equilibrium distance. A conjugate gradient minimization algorithm was utilized to relax the superposition of atoms generated in the box construction process. A subsequent 2 ns equilibration MD simulation was performed, where the protein backbone atoms were restrained with 10 kcal/mol Å^2. Finally, a 50 ns MD simulation was performed for data acquisition. Following the simulations, the tool *g_cluster* from the GROMACS package (Pronk et al., 2013) was used to perform a cluster analysis in 2500 conformations of albumin, taken at intervals of 20 ps from the 50 ns trajectory. The gromos algorithm (Daura et al., 1999), using a cutoff of 2 Å, was used to generate the clusters. The RMSD was calculated between all the structures and superimposed considering only non-hydrogen atoms.

2.8. Molecular modeling calculation

The HSA structures used in the molecular modeling calculations were obtained from the cluster analysis performed by the molecular dynamic simulations. The three-dimensional structure of the 2PHE molecule was obtained from the Gaussian 09 program (Frisch et al., 2009). AutoDockTools (ADT) (Sanner, 1999) was used to prepare the HSA and 2PHE by merging non-polar hydrogen atoms, adding partial charges and atom types. The ligand rigid root was generated automatically, setting all possible rotatable bonds defined as active by torsions (2PHE has 1 torsion). Grid maps were generated with 0.375 Å spacing and the dimensions of 60 × 60 × 60 points by the AutoGrid 4.2 program (Morris et al., 1998). These maps were centered on Sites 1 and 2 of the HSA structures. The AutoDock 4.2 program (Morris et al., 1998) was employed to study the binding site between 2PHE and HSA by applying the Lamarckian Genetic Algorithm (LGA) for minimization where the number of energy evaluations was 2.5 million, population size was 150 and root-square-mean deviation (RMSD) tolerance for cluster analysis was 2.0 Å. Random starting positions on the entire protein surface and random orientations were used for the ligand (2PHE). For each docking simulation, 100 different conformers were generated. The structural representation was prepared using PyMOL (Delano, 2002) and the map of interaction was calculated using LigPlot (Wallace, Laskowski, & Thomton, 1995).

2.9. Accessible surface area calculations

The accessible surface area (ASA) of uncomplexed HSA and its docked complexes with 2PHE were calculated using the NACCESS program (Hubbard & Thornton, 1993). The HSA–2PHE complex structures were obtained from the best molecular modeling structure and changes in absolute ASA for residue i were calculated using the following equation:

$$\Delta\mathrm{ASA}^i = \mathrm{ASA}^i_{\mathrm{uncomplexed}} - \mathrm{ASA}^i_{\mathrm{complexed}} \quad (2)$$

where $\mathrm{ASA}^i_{\mathrm{uncomplexed}}$ and $\mathrm{ASA}^i_{\mathrm{complexed}}$ is the absolute accessible surface area for free and complexed HSA residues, respectively. If one residue loses more than 10 Å^2 of absolute ASA going from the uncomplexed to the complexed state, it is considered to be involved in the interaction.

3. Results and discussions

3.1. Fluorescence quenching process of HSA by 2-phenylchromone

The fluorescence quenching process can occur when the intensity of the fluorescence signal decreases. Various molecular interactions may result in quenching, among them reactions with the excited state, molecular rearrangement, energy transfer, ground state complex formation and collisional quenching. These different mechanisms are usually classified as either dynamic or static. In addition, quenching mechanisms can be distinguished by their dependence on temperature and viscosity, or preferably by measuring the fluorescence lifetime. Higher temperatures result in faster diffusion and therefore a larger extension of collisional quenching. But higher temperatures also imply a dissociation of the weakly bound complex, leading to a less static quenching process (Lakowicz, 1999). The fluorescence intensity of the HSA decreased with an increasing 2PHE concentration (Fig. 1a), indicating that the microenvironment of the single tryptophan residue (Trp214) of the HSA is affected by the presence of the 2PHE. The effect of ethanol on the fluorescence intensity of HSA is negligible (Supplementary material, Fig. S1).

Data analysis regarding the fluorescence quenching process was performed by applying the Stern–Volmer equation (Lakowicz, 1999):

$$F_0/F = 1 + K_q\tau_0[Q] = 1 + K_{SV}[Q] \quad (3)$$

where F_0 and F are the steady-state fluorescence intensities in the absence and presence of a quencher (Q), respectively. K_q is the bimolecular quenching constant, τ_0 is the fluorophore lifetime in the absence of quencher, whose value for HSA is 10^{-8} s (Lakowicz, 1999), [Q] is the quencher concentration and K_{SV} is the Stern–Volmer quenching constant. In the investigated concentration range, the results of fluorescence quenching at 288, 298 and 308 K are in accordance with the Stern–Volmer equation (Supplementary material, Fig. S2).

The results in Table 1 show that the Stern–Volmer constant values are very close ($1.3 \times 10^5\ M^{-1}$) even with the temperature increment, such that the K_{SV} constants were temperature independent. Thus, evaluations of the K_q constants and the absorption spectrum of the fluorophore were performed to elucidate the quenching mechanism involved in the HSA–2PHE interaction. The bimolecular quenching constant values that were calculated by Eq. (3) are greater than $2.0 \times 10^{10}\ M^{-1}\ s^{-1}$, which represents the maximum diffusion collision rate for various quenchers with biopolymers. In addition, the absorption spectrum of the HSA presented changes in the presence of 2PHE (Supplementary material, Fig. S3). Consequently, the quenching mechanism of the HSA–2PHE interaction should follow the static process (ground state complex) (Lakowicz, 1999).

3.2. Analysis of binding equilibria

For the static quenching mechanism, the binding constant (K_b) and the number of binding sites (n) can be calculated using the following equation (Bi et al., 2004):

$$\log(F_0 - F)/F = n \log K_b - n \log(1/([D_0] - (F_0 - F)[P_0]/F)) \quad (4)$$

where [D_0] and [P_0] are the drug (2PHE) and protein (HSA) total concentration, respectively.

Fig. 1b shows the binding equilibrium plots for the fluorescence quenching of HSA by 2PHE at 288, 298 and 308 K. The dependence of $\log[(F_0 - F)/F]$ on the value of $\log(1/([D_0] - (F_0 - F)[P_0]/F))$ is linear, with a slope equal to the value of n and the value $n \log K_b$ fixed on the ordinate. For the HSA–2PHE complex, and n values at 288, 298 and 308 K are shown in Table 1. It was observed that the number of binding sites of the complex is approximately equal to 1.0. Neither K_b values nor values had relevant changes with increasing temperature.

Table 1
Stern–Volmer quenching constant (K_{SV}), bimolecular quenching constant (K_q), binding constant (K_b), and binding site numbers (n) of the interaction between HSA and 2PHE at pH 7.0 and 288, 298 and 308 K.

T (K)	K_{SV} ($\times 10^5\ M^{-1}$)	K_q ($\times 10^{14}\ M^{-1}\ s^{-1}$)	K_b ($\times 10^5\ M^{-1}$)	n
288	1.29	1.29	1.80	0.92
298	1.31	1.31	1.79	0.91
308	1.31	1.31	1.77	0.93

The correlation coefficient is $\geqslant 0.995$.

3.3. Thermodynamic analysis

The driving forces responsible for the interaction between HSA and 2PHE were calculated using the van't Hoff equation:

$$\ln K_b = -\frac{\Delta H^\circ}{RT} + \frac{\Delta S^\circ}{R} \quad (5)$$

where ΔH° is the enthalpy change, ΔS° is the entropy change, R is the universal gas constant and is the binding constant at the correspondent temperature (T). Table 2 shows ΔH° and ΔS° values obtained through the slope and the ordinate of the van't Hoff relationship (insert Fig. 1b), with the respective values of Gibbs free energy changes (ΔG°) as calculated with the Eqs. (5) and (6) in the temperature range of 288–308 K:

$$\Delta G^\circ = \Delta H^\circ - T\Delta S^\circ \quad (6)$$

The values of $\Delta G^\circ < 0$ indicated that the interaction process is spontaneous. For the HSA–2PHE complex, the results of thermodynamic analysis showed that ΔH° is very small and $\Delta S^\circ > 0$. The favorable entropic term ($-T\Delta S^\circ$) provided the major contribution for ΔG°, characterizing an entropically driven reaction. The present results therefore indicate that the forces which motivate the binding can be classified as a classical hydrophobic interaction (Kauzmann, 1959; Nemethy & Scheraga, 1962; Tanford, 1973), verified elsewhere for the interaction between HSA and porphyrins (Rotenberg, Cohen, & Margalit, 1987). The hydrophobic contribution may be a keystone in the interaction between HSA and 2PHE. In the meantime, it is not the only intermolecular interaction which contributes to complex stability, and it is also necessary to consider the electrostatic contribution (Ross & Subramanian, 1981).

3.4. Binding density function method

The thermodynamic basis for the binding density function (BDF) method is that the distribution of bound ligands per macromolecule in i different states (Σv_i) is strictly determined at equilibrium by the free ligand concentrations (L_F). Thus, if L_F is the same for two (or more) solutions at different total macromolecule concentrations (M_T), then Σv_i will also be the same in each solution. As a result, constant values of L_F and Σv_i will exist for a number

Table 2
Thermodynamic parameters of the HSA–2PHE complex at pH 7.0 and 288, 298 and 308 K.

T (K)	ΔH° (kJ mol^{-1})	ΔG° (kJ mol^{-1})	ΔS° (J mol^{-1} K^{-1})	R
288	−0.6	−28.9	98.4	
298		−29.9		0.978
308		−30.9		

R is the correlation coefficient.

of different combinations of total ligand (L_T) and total macromolecule (M_T) concentrations, which satisfy the mass conservation equation (Lohman & Bujalowski, 1991):

$$L_T = L_F + (\Sigma \nu_i) M_T \quad (7)$$

Considering the general relationship between the concentration of each macromolecule species with i bound ligands and the experimentally observed signal (S_{obs}) from the macromolecule, the fractional signal molar changes (ΔS_{obs}) observed in the presence of L_T and M_T will be given by:

$$\Delta S_{obs} = (S_{obs} - S_F M_T)/S_F M_T \quad (8)$$

where $S_F M_T$ is the observed signal for a free macromolecule in the absence of a ligand (F_0, see Section 3.1). Thus, for fluorescence quenching, experiments have to be $\Delta S_{obs} = (F - F_0)/F_0$ (Lohman & Bujalowski, 1991). A horizontal line was drawn intersecting the three titration curves in Fig. 2a, defining a constant value of ΔS_{obs} and three sets of (L_{Tx}; M_{Tx}) (x = 1, 2 and 3) for which L_F and $\Sigma \nu_i$ were constants (see insert in Fig. 2a).

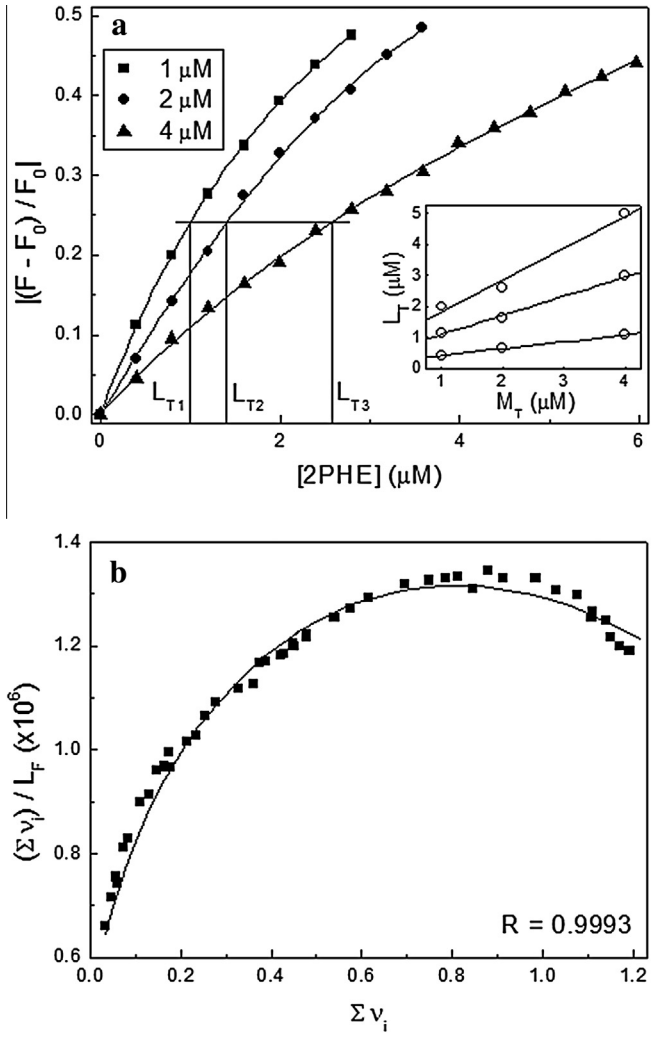

Fig. 2. (a) Titrations of 2PHE in HSA solutions, as monitored by fluorescence quenching of the Trp214 residue in HSA for three different protein concentrations at pH 7.0 and 298 K. L_{T1}, L_{T2} and L_{T3} represent the total ligand concentrations for the constant fractional signal molar change value of three different total protein concentrations (M_{T1}, M_{T2} and M_{T3}). The insert corresponds to only three sets of concentration pairs (L_T; M_T) to exemplify the utilization of Eq. (7) obtaining $\Sigma \nu_i$ and L_F values. (b) Scatchard plot for the binding between 2PHE and HSA generated from BDF method. The solid line shows fit of the experimental data using Eq. (11) and R is the correlation coefficient.

From the L_F and $\Sigma \nu_i$ values obtained from Eq. (7), the Scatchard plot for the binding between HSA and 2PHE can be built without the use of any binding model *a priori*. The Scatchard plot showed a downward curvature (Fig. 2b), indicating that the HSA–2PHE complex presents a positive cooperativity, which means that the binding at the first site enhances the affinity of the second one. The interaction between HSA and 2PHE was fitted using a global binding model in which the macromolecule contains two binding sites for a ligand. The reaction mechanism for this binding model can be described as follows (Di Cera, 1995):

$$M + L \overset{k_1}{\Longleftrightarrow} ML \quad (9)$$

$$ML + L \overset{k_2}{\Longleftrightarrow} ML_2 \quad (10)$$

where k_1 and k_2 are stepwise binding constants, which can be obtained from the following equation:

$$\sum \nu_i = \left(2k_1 L_F + 2k_1 k_2 L_F^2\right) / \left(1 + 2k_1 L_F + k_1 k_2 L_F^2\right) \quad (11)$$

The obtained values for k_1 and k_2 were 2.42×10^5 and $6.90 \times 10^6\ M^{-1}$, respectively. The k_1 value is in accordance with the results obtained from the analysis of binding equilibria (Section 3.2). The discrepancy between the number of binding sites found by BDF and binding equilibria analysis may be due to inherent constraints in the last model, according to Eq. (4). The Hill coefficient calculated using $n_H = 2/(1 + \sqrt{k_1/k_2})$ was 1.68, indicating that the interaction between HSA and 2PHE exhibits a positive cooperative as previously mentioned. The maximum binding capacity curve of HSA presented a corresponding 2PHE concentration of 0.76 μM (Supplementary material, Fig. S4).

3.5. Identification of the binding sites of 2-phenylchromone on HSA by drug displacement

The determination of the binding site location of 2PHE on HSA was performed using the competitive binding assay between 2PHE and specific site markers, namely, warfarin (WAR), ibuprofen (IBU) and methyl orange (MTO) for Sites 1, 2 and 3, respectively (Peters, 1996; Zsila, 2013). To probe the binding site of 2PHE on HSA, the fluorescence quenching rate (F/F_0) in the absence and presence of markers was compared, and are presented in Fig. 3. The quenching rate for 2PHE decreased in the presence of WAR (Site 1 marker), increased in the presence of IBU (Site 2 marker)

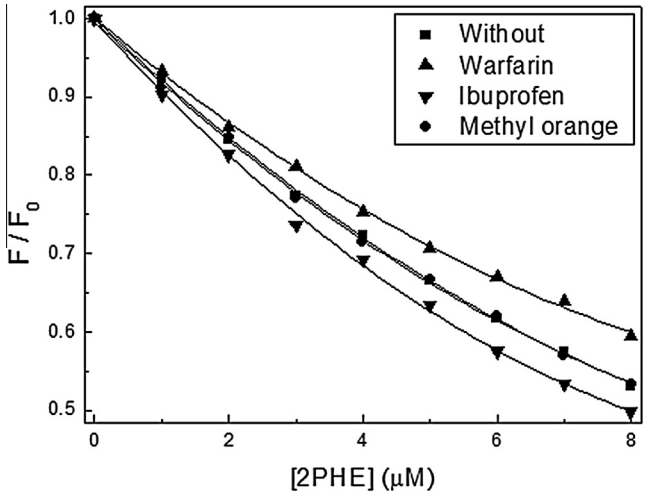

Fig. 3. Fluorescence quenching rates of HSA by 2PHE in the absence and presence of specific site markers (warfarin, ibuprofen or methyl orange). [HSA] = [Marker] = 4.0 μM, pH 7.0, T = 298 K, and λ_{ex} = 295 nm.

and remained the same in the presence of MTO (Site 3 marker), when compared with the quenching rate for 2PHE with no marker. The results suggest that 2PHE binds to Site 1 and Site 2 of HSA, which are located in subdomain IIA and IIIA, respectively. The identification of the two binding sites for 2PHE on HSA corroborates the result obtained by the BDF method (Section 3.4).

3.6. Ab initio calculation

The optimization and vibrational calculation performed for the 2PHE with the DFT/B3LYP/6-311++G(2d,p) method showed that the optimized structure is stable (global minimum on the potential energy surface) since no imaginary frequency was obtained. Some calculated bond distances, bond angles, and dihedral angles are presented in Table S1 of Supplementary material. The results of the TD-DFT calculation were in agreement with the experimental UV–Vis absorbance data (Supplementary material, Table S2), since the maximum experimental UV–Vis absorbance corresponds to the vertical transition according to the Franck–Condon principle. The results of *ab initio* calculations for 2PHE were therefore consistent with the experimental data.

From the MEP of 2PHE (Supplementary material, Fig. S7) it was possible to detect the existence of a neutral charge distribution on the planar faces of the rings of the molecule. A dense distribution of negative charges can also be seen near the O4 oxygen atom, while a slightly positive electrostatic potential is localized close to all the hydrogen atoms in the flavonoid.

3.7. Molecular dynamic and molecular modeling calculations

Molecular modeling results are highly modulated by the receptor structure used because, typically, this structure is kept rigid

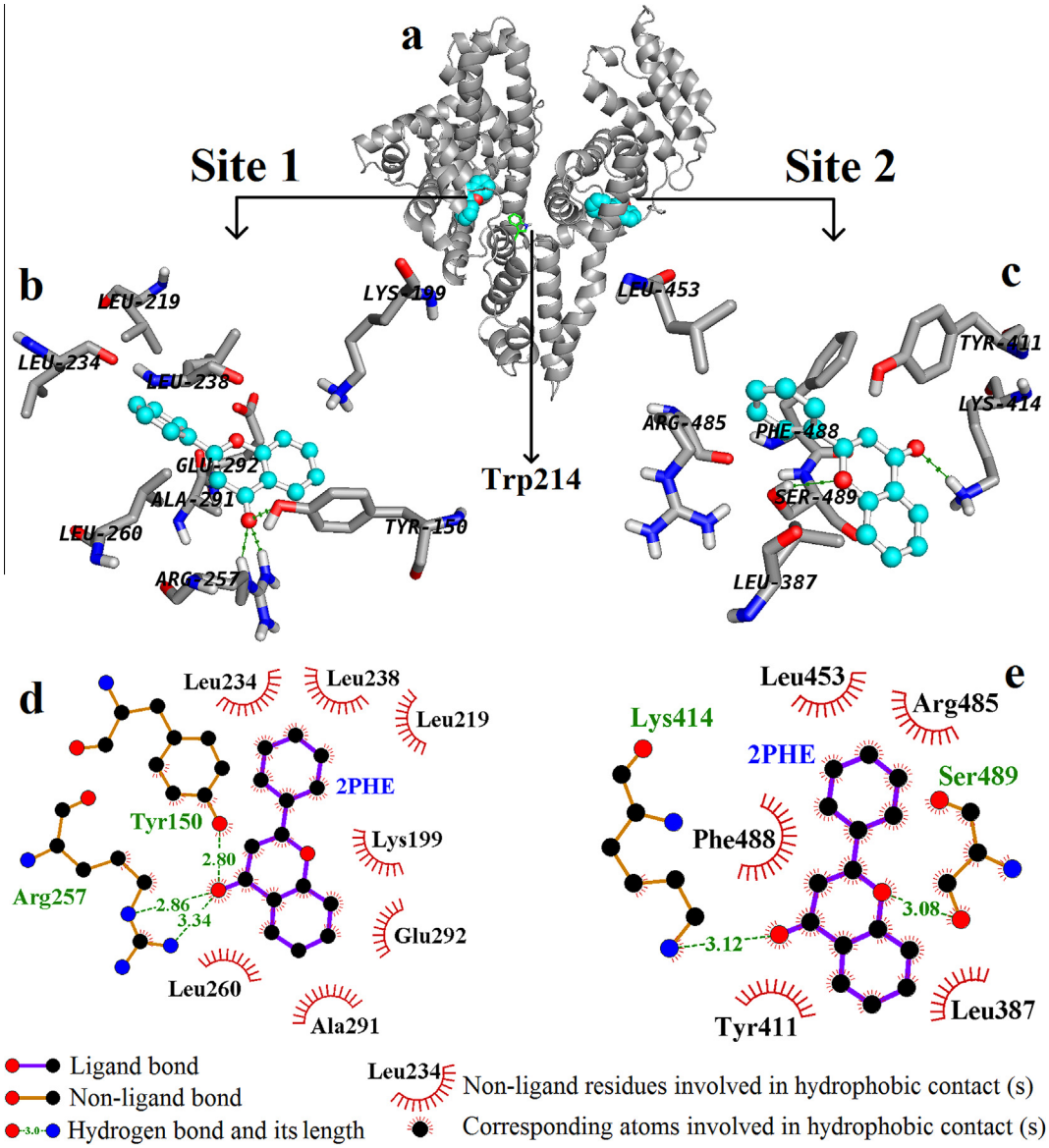

Fig. 4. (a) Location of the 2PHE molecules in the subdomain IIA (Site 1) and IIIA (Site 2) of the fourth cluster of HSA, close to the single tryptophan residue (Trp214). The protein is shown as a cartoon and 2PHE molecules as spheres. Three-dimensional structural detail of the microenvironment interaction of 2PHE with (b) Site 1 and (c) Site 2 of HSA obtained by molecular modeling calculations. 2PHE molecules are shown as stick and ball models, the amino acid residues are denoted as stick models (C, gray; O, red; N, blue; H, white), and the hydrogen bonds depicted by green dotted line. Two-dimensional representation of the interaction maps between 2PHE and residues of (d) Site 1 and (e) Site 2 of HSA. The structural representation was prepared using PyMOL (Delano, 2002) and the map of interactions was calculated using LigPlot (Wallace et al., 1995). (For interpretation of the references to color in this figure legend, the reader is referred to the web version of this article.)

during the calculations. Thus, the direct use of crystallographic structures in these calculations can generate spurious results since the solid state chemical environment does not match the physiological one, and this reflects in the protein structure, particularly on the conformation of the side-chains. To avoid these, molecular dynamic simulations of crystallographic HSA structure in an aqueous solution with physiological ionic strength (NaCl 150 mM) and pH = 7.0, were performed to generate the receptor conformations to be used in the molecular docking calculations. These structures were acquired from the obtained trajectory by cluster analysis. This procedure generated six clusters, and the most representative conformation of each was used in molecular docking calculations to study the interaction of the 2PHE with Sites 1 and 2 of HSA, based upon the drug displacement experiments (Section 3.5.). The best theoretical binding energies (ΔG_B) for the Sites 1 and 2 of the six HSA clusters were calculated, as well as their corresponding theoretical binding constants (K_B), determined by $K_B = \exp(-\Delta G_B/RT)$ (Supplementary material, Table S3). Among the six HSA clusters, the fourth cluster presented a theoretical binding energy and constant values (Table S3) in agreement with the binding equilibria analysis (K_b, Section 3.2.) and binding density function method (K_a, Section 3.4.).

Fig. 4 summarizes the interaction between human serum albumin and 2PHE from three different perspectives. At the top, Fig. 4a shows the tertiary structure of the protein with Site 1 on the left side, the Trp214 residue roughly positioned in between, and Site 2 on the right side. In the middle, Fig. 4b and c show the molecular microenvironment with the closest amino acid participants of the complex. At the bottom, Fig. 4d and e show in detail all the non covalent interactions responsible for stabilizing the complex. These results were obtained based on the fourth most representative cluster, which fits energetically with the experimental data. On the left branch (Fig. 4b) the closest residues interacting with 2PHE are: Lys119, Leu (219, 234, 238 and 260), Ala291, Glu292, Arg257 and Tyr150. While, on the right branch (Fig. 4c), the closest residues taking part in the interactions with 2PHE are: Leu (387 and 453), Arg485, Phe488, Ser489, Tyr411 and Lys414. Finally, using the LigPlot program (Wallace et al., 1995), it was possible to underline the residues which are crucial in stabilizing the complex. At Site 1 (Fig. 4d), Lys199, Leu (219, 234, 238 and 260), Ala291, and Glu292 are residues involved in the hydrophobic interactions with 2PHE. The residues Arg257 and Tyr150 formed hydrogen bonds with the O4 oxygen atom from the 2PHE molecule. It should be noted that the oxygen atom is positioned at the densest negative charge distribution, as can be seen at the MEP of the flavonoids (Fig. S7). The NH_2 and NH groups of the Arg257 side chain built two hydrogen bonds with 2PHE, at distances of 3.34 and 2.86 Å, respectively. The OH group of the Tyr150 side chain forms a hydrogen bond with 2PHE, with a length of 2.80 Å. At Site 2 (Fig. 4e) residues Leu387, Tyr411, Leu453, Arg485 and Phe488 performed hydrophobic interactions with the 2PHE. The Lys414 and Ser489 residues form hydrogen bonds with 2PHE, presenting formation distances of 3.12 and 3.08 Å, respectively. The group NH_2 of Lys side chain makes up a hydrogen bond with the O4 oxygen atom of 2PHE (the most electronegative atom of the flavonoid, see Fig. S7). The OH group of Ser489 side chain set up a hydrogen bond with the O1 oxygen atom of 2PHE.

The molecular dynamic and docking results indicate that the hydrophobic contribution is the major interaction involved in the binding microenvironment of the Sites 1 and 2 of HSA with 2PHE. In addition, the electrostatic interactions also contribute to the complex formation, stabilizing the binding with hydrogen bonds. This set of results is in agreement with the thermodynamic analysis (Section 3.3.).

3.8. Accessible superficial area calculation

The average area lost by HSA residues in the complex formation with 2PHE was approximately 21 and 22 $Å^2$ at Sites 1 and 2, respectively. Ala291 and Ser489 were the residues with the greatest loss of ASA in Sites 1 and 2, respectively (Supplementary material, Table S4). ASA changes for nonpolar and polar atoms of the residues involved in the HSA–2PHE complex formation were 70 and 30% at Site 1, 50 and 50% at Site 2, and 61 and 39% at both of the two sites together, respectively. ASA analysis suggests that hydrophobic interactions are a major contribution in the binding of 2PHE with HSA; however, electrostatic interactions also have a considerable contribution. This result is in accordance with the experimental data.

4. Conclusion

The interaction between 2-phenylchromone and HSA was investigated using fluorescence, UV–Visible and circular dichroism spectroscopy, along with computational methods, such as *ab initio*, molecular dynamic and molecular modeling calculations. Fluorescence and UV–Visible data analysis indicated that the main quenching mechanism is static. The analysis of binding equilibria demonstrated that the binding constant for 2PHE with HSA has a moderate affinity, having a balanced behavior not so low as to avoid dispensation and not too high to prevent the decrement of the blood plasma concentration. This moderate affinity provides an appropriate condition for uniformly efficient distribution of 2PHE by HSA in the blood circulatory system to reach target organs. The $\Delta G^\circ < 0$ value indicates that the binding process is spontaneous, and ΔH° very close to zero and the $\Delta S^\circ > 0$ values suggest that the hydrophobic interaction is the main contribution involved in the HSA–2PHE complex formation. Although the electrostatic interaction at first glance would be neglected it is still important in stabilizing the binding complex. The Scatchard plot obtained by the BDF method showed a downward curvature, indicating that the HSA–2PHE complex presents positive cooperativity. The fit of this binding isothermal suggests that two molecules of 2PHE bind to HSA, which was confirmed by the drug displacement experiments, showing that the subdomain IIA (Site 1) and IIIA (Site 2) were the most probable binding sites in HSA. The distance between donor (HSA-Trp214) and acceptor (2PHE) calculated by FRET was 1.982 nm, suggesting that a transfer of energy may possibly occur between them. From CD spectroscopy analysis, no significant change in secondary structure due to the complex formation was observed (Supplementary material). The molecular dynamic and modeling calculations indicated that the 2PHE as a whole matches its molecular architecture (MEP) with Sites 1 and 2 of HSA. The computational results indicated that hydrophobic interactions are the principal contribution in the HSA–2PHE complex formation and the electrostatic interactions (hydrogen bond) are important in the stabilization of the binding complex, which is in agreement with the experimental results.

Acknowledgments

The author I.P.C. gratefully acknowledges a CAPES scholarship and financial support received from FAPESP. I.P.C. also recognizes GridUNESP for the availability of Gaussian 09 quantum chemical program, and Prof. Dr. Márcio Francisco Colombo for the use of the UV–Vis spectrometer.

The author ASdA thanks for the grant #2010/18169-3 (FAPESP) and CENAPAD-SP (Centro Nacional de Processamento de Alto Desempenho em São Paulo).

Appendix A. Supplementary data

Supplementary data associated with this article can be found, in the online version, at http://dx.doi.org/10.1016/j.foodchem.2015.10.027.

References

Best, R. B., Zhu, X., Shim, J., Lopes, P. E. M., Mittal, J., Feig, M., & MacKerell, A. D. Jr., (2012). Optimization of the additive CHARMM all-atom protein force field targeting improved sampling of the backbone ϕ, ψ and side-chain $\chi 1$ and $\chi 2$ dihedral angles. *Journal of Chemical Theory and Computation, 8*, 3257–3273.

Bi, S., Ding, L., Tian, Y., Song, D., Zhou, X., Liu, X., & Zhang, H. (2004). Investigation of the interaction between flavonoids and human serum albumin. *Journal of Molecular Structure, 703*, 37–45.

Borissevitch, I. E. (1999). More about the inner filter effect: corrections of Stern–Volmer fluorescence quenching constants are necessary at very low optical absorption of the quencher. *Journal of Luminescence, 81*, 219–224.

Bravo, L. (1998). Polyphenols: Chemistry, dietary sources, metabolism, and nutritional significance. *Nutrition Reviews, 56*, 317–333.

Caruso, I. P., Vilegas, W., Fossey, M. A., & Cornélio, M. L. (2012). Exploring the binding mechanism of Guaijaverin to human serum albumin: Fluorescence spectroscopy and computational approach. *Spectrochimica Acta Part A: Molecular and Biomolecular Spectroscopy, 97*, 449–455.

Caruso, I. P., Vilegas, W., Souza, F. P., Fossey, M. A., & Cornélio, M. L. (2014). Binding of antioxidant flavone isovitexin to human serum albumin investigated by experimental and computational assays. *Journal of Pharmaceutical and Biomedical Analysis, 98*, 100–106.

Daura, X., Gademann, K., Jaun, B., Seebach, D., van Gunsteren, W. F., & Mark, A. E. (1999). Peptide folding: When simulation meets experiment. *Angewandte Chemie International Edition, 38*, 236–240.

Delano, W. L. (2002). *The PyMOL molecular graphics system*. San Carlos, CA,USA: DeLano Scientific.

Di Cera, E. (1995). *Thermodynamic theory of site-specific binding processes biological macromolecules*. Cambridge: Cambridge University Press.

Frisch, M. J., Trucks, G. W., Schlegel, H. B., Scuseria, G. E., Robb, M. A., Cheeseman, J. R., ... Fox, D. J. (2009). *Gaussian 09, revision A.02*. Wallingford, CT: Gaussian Inc.

Grotewold, E. (2006). *The science of flavonoids*. New York: Springer.

Hubbard, S. J., & Thornton, J. M. (1993). *NACCESS*. London: Computer Program, Department of Biochemistry and Molecular Biology, University College.

Jorgensen, W. L., Chandrasekhar, J., Madura, J. D., Impey, R. W., & Klein, M. L. (1983). Comparison of simple potential functions for simulating liquid water. *Journal of Chemical Physics, 79*, 926–935.

Jung, J., Ishida, K., Nishikawa, J., & Nishihara, T. (2007). Inhibition of estrogen action by 2-phenylchromone as AhR agonist in MCF-7cells. *Life Sciences, 81*, 1446–1451.

Kauzmann, W. (1959). Factor in interpretation of protein denaturation. *Advances in Protein Chemistry, 14*, 1–63.

Lakowicz, J. R. (1999). *Principles of fluorescence spectroscopy* (2nd ed.). New York: Kluwer Academic Publishers/Plenum Press.

Lohman, T. M., & Bujalowski, W. (1991). Thermodynamic methods for model-independent determination of equilibrium binding isotherms for protein–DNA interactions: Spectroscopic approaches to monitor binding. *Methods in Enzimology, 208*, 158–290.

Mennucci, B., Cancès, E., & Tomasi, J. (1997). Evaluation of solvent effects in isotropic and anisotropic dielectrics, and in ionic solutions with a unified integral equation method: Theoretical bases, computational implementation and numerical applications. *Journal of Physical Chemistry B, 101*, 10506–105017.

Morris, G. M., Goodsell, D. S., Halliday, R. S., Huey, R., Hart, W. E., Belew, R. K., & Olson, A. J. (1998). Automated docking using a Larmarckian genetic algorithm and an empirical binding free energy function. *Journal of Computational Chemistry, 19*, 1639–1662.

Najmus-Saqib, Q., Alam, F., & Ahmad, M. (2009). Antimicrobial and cytotoxicity activities of the medicinal plant *Primula macrophylla*. *Journal of Enzyme Inhibition and Medicinal Chemistry, 24*, 697–701.

Nemethy, G., & Scheraga, H. A. (1962). Structure of water and hydrophobic binding in proteins. II. Model for the thermodynamic properties of aqueous solutions of hydrocarbons. *Journal of Chemical Physics, 36*, 3401–3417.

Peters, T. (1996). All about albumin. *Biochemistry, genetics and medical application*. Academic Press: San Diego.

Phillips, J., Braun, R., Wang, W., Gumbart, J., Tajkhorshid, E., Villa, E., ... Schulten, K. (2005). Scalable molecular dynamics with NAMD. *Journal of Computational Chemistry, 26*, 1781–1802.

Pohjala, L., & Tammela, P. (2012). Aggregating behavior of phenolic compounds – A source of false bioassay results? *Molecules, 17*, 10774–10790.

Pronk, S., Páll, S., Schulz, R., Larsson, P., Bjelkmar, P., Apostolov, R., ... Lindahl, E. (2013). GROMACS 4.5: A high-throughput and highly parallel open source molecular simulation toolkit. *Bioinformatics, 29*, 845–854.

Ross, P. D., & Subramanian, S. (1981). Thermodynamics of protein association reactions: Forces contributing to stability. *Biochemistry, 20*, 3096–3102.

Rotenberg, M., Cohen, S., & Margalit, R. (1987). Thermodynamics of porphyrin binding to serum albumin: Effects of temperature, of porphyrin species and of albumin-carried fatty acids. *Photochemistry and Photobiology, 46*, 689–693.

Sanner, M. F. (1999). Python: A programming language for software integration and development. *Journal of Molecular Graphics and Modelling, 17*, 57–61.

Sinisi, V., Forzato, C., Cefarin, N., Navarini, L., & Berti, F. (2015). Interaction of chlorogenic acids and quinides from coffee with human serum albumin. *Food Chemistry, 168*, 332–340.

Sreerama, N., & Woody, R. W. (2000). A self-consistent method for the analysis of protein secondary structure from circular dichroism. *Analytical Biochemistry, 282*, 252–260.

Sugio, S., Kashima, A., Mochikuzi, S., Noda, M., & Kobayashi, K. (1999). Crystal structure of human serum albumin at 2.5 Å resolution. *Protein Engineering, 12*, 439–446.

Tanford, J. (1973). *The theory of the hydrophobic effect*. New York: Wiley.

Wallace, A. C., Laskowski, R. A., & Thomton, J. M. (1995). LIGPLOT: A program to generate schematic diagrams of protein-ligand interaction. *Protein Engineering, 8*, 127–134.

Wu, D., Yan, J., Wang, J., Wang, Q., & Li, H. (2015). Characterization of interaction between food colourant allura red AC and human serum albumin: Multispectroscopic analyses and docking simulations. *Food Chemistry, 170*, 423–429.

Zsila, F. (2013). Subdomain IB is the third major drug binding region of human serum albumin: Toward the three-sites model. *Molecular Pharmaceutics, 10*, 1668–1682.